Redox Biology 11 (2017) 524–534

Contents lists available at ScienceDirect

Redox Biology

journal homepage: www.elsevier.com/locate/redox

Research Paper

# Tert-butyl hydroperoxide (t-BHP) induced apoptosis and necroptosis in endothelial cells: Roles of NOX4 and mitochondrion

Wenwen Zhao[a], Haitao Feng[a], Wen Sun[a], Kang Liu[b], Jin-Jian Lu[a], Xiuping Chen[a,*]

[a] State Key Laboratory of Quality Research in Chinese Medicine, Institute of Chinese Medical Sciences, University of Macau, Macao, China
[b] Department of Pharmacology of Chinese Materia Medica, China Pharmaceutical University, Nanjing, PR China

ARTICLE INFO

*Keywords:*
Apoptosis
Necroptosis
Reactive oxygen species
NOX4
Mitochondria
Endothelial cells

ABSTRACT

Oxidative stress causes endothelial death while underlying mechanisms remain elusive. Herein, the pro-death effect of tert-butyl hydroperoxide (t-BHP) was investigated with low concentration (50 μM) of t-BHP (t-$BHP_L$) and high concentration (500 μM) of t-BHP (t-$BHP_H$). Both t-$BHP_L$ and t-$BHP_H$ induced endothelial cell death was determined. T-$BHP_L$ induced caspase-dependent apoptosis and reactive oxygen species (ROS) generation, which was inhibited by N-acetyl-L-cysteine (NAC). Furthermore, NADPH oxidase inhibitor diphenyleneiodonium (DPI), NOX4 siRNA, and NOX4 inhibitor GKT137831 reduced t-$BHP_L$-induced ROS generation while mitochondrial respiratory chain inhibitors rotenone (Rot), 2-thenoyltrifluoroacetone (TTFA), and antimycin A (AA) failed to do so. NOX4 overexpression resulted in increased ROS generation and Akt expression but decreased sensitivity to t-$BHP_L$. In contrast, T-$BHP_H$ induced LDH release, PI uptake, and cell translucent cytoplasm. RIP1 inhibitor necrostatin-1 (Nec-1), MLKL inhibitor necrosulfonamide (NSA) and silencing RIP1, RIP3, and MLKL inhibited t-$BHP_H$-induced cell death while pan-caspase inhibitor Z-VAD-FMK showed no effect. T-$BHP_H$-induced ROS production was inhibited by TTFA, AA and Rot while DPI showed no effect. T-$BHP_H$ induced RIP1/RIP3 interaction, which was decreased by Rot, TTFA, and AA. Silence RIP1 and RIP3 but not MLKL inhibited t-$BHP_H$-induced mitochondrial membrane potential (MMP) decrease and ROS production. Moreover, P38MAPK inhibitor SB203580 reversed both t-$BHP_L$ and t-$BHP_H$-induced cell death while inhibitors for ERKs and JNKs showed no obvious effect. These data suggested that t-BHP induced both apoptosis and necroptosis in endothelial cells which was mediated by ROS and p38MAPK. ROS derived from NADPH oxidase and mitochondria contributed to t-$BHP_L$ and t-$BHP_H$-induced apoptosis and necroptosis, respectively.

## 1. Introduction

Cell death is a fundamental feature in the lifespan of all the metazoans. Both passive cell death caused by severe structural damage and active cell death owing to confined biological disruptions could happen. The former is uncontrolled while the latter is tightly regulated [1]. Apoptosis is the first-identified form of regulated cell death and was considered as the sole form of regulated cell death for decades [2]. However, accumulated research has identified a few previously unrecognized, regulated cell death models such as regulated necrosis, autophagic cell death. Regulated necrosis is defined as a genetically controlled necrosis with characterized morphology of cytoplasmic granulation, organelle and/or cellular swelling [3]. Although parthanatos, oxytosis, ferroptosis, NETosis, pyronecrosis, and pyroptosis have been considered as different types of regulated necrosis [3], necroptosis is the most understood form of regulated necrotic cell death routine. Though it is morphologically difficult to distinguish necrosis and necroptosis, necroptosis is tightly regulated and genetically controlled by receptor-interacting protein kinase 1 (RIP1), RIP3, and mixed lineage kinase domain-like protein (MLKL) pathways [2,4].

Endothelial cells, the single layer of cells lining all the vasculatures, exert multiple actions such as regulation of vascular permeability and tone, blood fluid and flow, coagulation and fibrinolysis, leukocyte activation, inflammatory, immune surveillance, and cell growth [5,6].

*Abbreviations:* AA, Antimycin A; ALL, Allopurinol; ASK1, Apoptosis-signaling kinase 1; $DCFH_2$-DA, 5-(6)-carboxy-2′, 7′-dichlorodihydrofluorescein diacetate; DPI, Diphenyleneiodonium; ERK, Extracellular signal regulated kinase; $H_2O_2$, Hydrogen peroxide; JNK, c-Jun-N-terminal kinase; MAPKs, Mitogen-activated protein kinases; MLKL, Mixed lineage kinase domain-like protein; MMP, Mitochondrial membrane potential; MTT, 3-(4,5-dimethyl-2-thiazolyl)-2,5-diphenyl-2-H-tetrazolium bromide; NAC, N-acetyl-L-cysteine; NOX4, NADPH oxidase 4; Nec-1, Necrostatin-1; NSA, Necrosulfonamide; PI, Propidium iodide; ROS, Reactive oxygen species; Rot, Rotenone; RIP1, Receptor-interacting protein 1; RIP3, Receptor-interacting protein 3; t-BHP, Tert-butyl hydroperoxide; t-$BHP_L$, Low concentration of t-BHP (50 μM); t-$BHP_H$, High concentration of t-BHP (500 μM); TTFA, 2-thenoyltrifluoroacetone;; XO, Xanthine oxidase; Z-VAD-FMK, Z-Val-Ala-DL-Asp-fluoromethylketone

* Corresponding author.
*E-mail address:* xpchen@umac.mo (X. Chen).

http://dx.doi.org/10.1016/j.redox.2016.12.036
Received 20 September 2016; Received in revised form 25 November 2016; Accepted 22 December 2016
Available online 05 January 2017

Endothelial dysfunction caused by endothelial injury and/or death is the initial step for a panel of vascular related diseases. Hyperglycemia, hyperlipidemia, hyperhomocysteinemia, smoking, inflammatory cytokines, shear stress, and environmental toxins etc are common inducers of endothelial death. Oxidative stress resulted from the overproduction of reactive oxygen species (ROS) might serve as one of the common mechanisms for them. In endothelial cells, multiple sources of ROS such as mitochondria, NADPH oxidase, xanthine oxidase (XO) etc have been identified [7,8]. The toxic roles of ROS in endothelial apoptosis has been widely recognized and deeply investigated. ROS activated apoptosis-signaling kinase 1 (ASK1) resulted in sustained JNK activation, which is a key step in initiating caspase-dependent apoptosis [5]. Recent evidence showed that ROS also contributes to TNF induced necroptosis in human colon adenocarcinoma HT-29 cells [9] while its role in endothelial cells remain unclear.

Hydrogen peroxide ($H_2O_2$), one of the major type of ROS, has been reported to induce necrosis dependent on PARP1 [10] while the role of RIP1 and RIP3 in $H_2O_2$ trigged necrosis remains controversial [11]. Although larger amount of exogenous $H_2O_2$ caused oncotic death in cultured endothelial cells, the cell death under this condition remains elusive. Still much less is known about the contribution of organelle-based ROS production in endothelial apoptosis and necroptosis. $H_2O_2$ is thermodynamically unstable and can easily decompose to form water and oxygen. Tert-butyl hydroperoxide (t-BHP), an organic peroxide widely used in a variety of oxidation processes, is widely used as a better alternative for $H_2O_2$ in oxidative stress studies. Herein, the pro-death effect of t-BHP on endothelial cells was studied and the underlying mechanisms were explored.

## 2. Materials and methods

### 2.1. Reagents

3-(4,5-dimethyl-2-thiazolyl)-2,5-diphenyl-2-H-tetrazolium bromide (MTT), 5-(6)- carboxy-2′, 7′-dichlorodihydrofluorescein diacetate ($DCFH_2$-DA), dimethyl sulfoxide (DMSO), Hoechst 33342, N-acetyl cysteine (NAC), diphenyleneiodonium chloride (DPI), rotenone (Rot), 2-thenoyltrifluoroacetone (TTFA), antimycin A (AA), allopurinol (ALL), and Akt Inhibitor VIII were purchased from Sigma-Aldrich (USA). LipofectamineTM 3000 was purchased from Life Technology (USA). Antibodies for NOX4, p22phox, and protein A/G PLUS-Agarose were purchased from Santa Cruz (USA). Antibodies for cleaved caspase 3 and caspase 7, phosphorylated ERK1/2 (p-ERK1/2), ERK1/2, phosphorylated p38MAPK (p-p38MAPK), p38MAPK, phosphorylated Akt (p-Akt), Akt, GAPDH, Histone H3, Bcl-2, RIP1, phosphorylated MLKL (p-MLKL), MLKL and $Na^+/K^+$ ATPase were purchased from Cell Signaling Technology (USA). RIP3 antibody was purchased from Abnova (USA). SiRNA for NOX4, RIP1, RIP3, and MLKL were purchased from Gene Pharma Company (China). Overexpression NOX4 plasmid was purchased from GeneChem Company (China). P5 Primary Cell 4D-Nucleofector® X Kit L (24 RCT) was purchased from Lonza Company (Switzerland). JC-1 kit and LDH Assay Kit were purchased from Beyotime (China). MitoSOX and MitoTracker were purchased from Invitrogen (USA). AlamarBlue Cell Viability Reagent was purchased from Thermo Fisher Scientific (USA).GKT137831 was purchased from BioChemPartner (China). FractionPREP™ Cell Fractionation Kit (for cell fraction extractions) was purchased from BioVision (USA). All other chemicals were purchased from Sigma-Aldrich (USA).

### 2.2. Cell culture

Human umbilical vein endothelial cells (HUVECs) were cultured in F-12K medium with 1.5 g/L sodium bicarbonate, 100 μg/ml heparin, 2 mM L-glutamine, 30 μg/mL endothelial cell growth supplement and 10% FBS at 37 °C in a humidified atmosphere of 5% $CO_2$. Tissue culture flasks, 96-well plates and 6-well plates were pre-coated with 0.2% gelatin. All assays were conducted using low cell passage cells (2–5 passages).

### 2.3. Cell viability assay

The cell viability was determined with MTT and alamarBlue assay. Cells were seeded in 96-well plates at a density of $1\times10^4$ cells/well and treated with t-BHP. For MTT assay, after treatment with t-BHP, cells were washed twice with PBS and incubated with 20 μL MTT (5 mg/ml in PBS) for 4 h. Then the culture medium was removed and DMSO (100 μL/well) was added. The absorbance was measured at 570 nm using a microplate reader (PerkinElmer, USA). For alamarBlue assay, t-BHP-treated cells were loaded with AlamarBlue Cell Viability Reagent (Thermo Fisher) [12] and incubated at 37 °C. After 6 h, plates were measured at 545 nm/590 nm (Ex/Em) using a Varioskan™ Flash Multimode Plate Reader (USA).

### 2.4. Apoptosis assay

Apoptosis was examined by human Annexin V/7AAD kit (BD Biosciences, USA) according to the manufacturer's instructions. Briefly, cells ($2.5\times10^5$) seeded in 6-well plates were treated with t-BHP with or without Z-VAD-FMK (1 μM) pretreatment. Then cells were harvested by incubation with Annexin V/FITC solution for 15 min at room temperature. The samples were immediately analyzed by flow cytometry using a FACSCanto™ system (BD Biosciences, USA). At least $1\times10^4$ cells were analyzed for each sample.

### 2.5. Caspase activity measurement

The activity of caspase 3/7 was measured by a commercial Caspase-Glo® 3/7 Assay Kit (Promega) following manufacturer's instructions.

### 2.6. Immunoprecipitation assay

After determination of the protein concentrations, the cell extracts were incubated with anti-RIP1 antibody (2 μg) for 2 h at 4 °C and followed by incubation with 20 μL of proteinA/G plus-agarose beads overnight. Then the beads were washed 3 times with ice-cold radio immunoprecipitation assay (RIPA) buffer and the bound proteins were extracted by adding 20 μL 2×SDS sample buffer and boiled for 5 min. The complexes were subjected to Western blotting.

### 2.7. Measurement of intracellular ROS

The production of t-BHP-induced ROS was measured by $DCFH_2$-DA probe as our previous report [13]. To explore the sources of ROS, cells were pretreated with DPI (1 μM), Rot (20 μM), TTFA (10 μM), AA (5 μM), or All (10 μM) for 1 h followed by t-BHP treatment for 30 min.

### 2.8. Mitochondrial membrane potential assay

The mitochondrial membrane potential (MMP) was assessed using a commercial kit following the manufacturer's instructions.

### 2.9. Measurement of mitochondrial ROS

Cells ($1\times10^4$ cells/well) cultured in 96-well plates were incubated with MitoTracker Green FM (100 nM) for 1 h at room temperature in an atmosphere of 5% $CO_2$. After treatment with t-BHP, cells were incubated with MitoSOX reagent working solution (1 μM) for 20 min at 37 °C. Fluorescence was observed with IN Cell Analyzer 2000 and quantified by a FACScan flow cytometer using the PE channel.

### 2.10. Immunofluorescence assay

Cells ($1\times10^4$ cells/well) cultured in 96-well plates were treated with t-BHP and then fixed with 4% PFA for 15 min at 4 °C. After permeabilized with PBS-T (containing 0.1% Triton x-100 in PBS solution) and blocked with PBS-B (containing 4% BSA in PBS solution), cells were incubated with the primary antibody (1:1000) and the secondary antibody (1:2000). The nucleus was stained with Hoechst 33342 in dark for 5 min and the fluorescence was observed with fluorescence microscope.

### 2.11. SiRNA knockdown

The NOX4, RIP1, RIP3, and MLKL were silenced with siRNAs and their sequences were as following:

| Genes | Target sequences of siRNA |
|---|---|
| NOX4 | 5′-ACUAUGAUAUCUUCUGGUA-3′ |
| RIP1 | 5′-AUCAAUCUGAGACUGUGUGAAGCCCdTdT-3′ |
| RIP3 | 5′-GCAGUUGUAUAUGUUAACGAGCGGUCGdTdT-3′ |
| MLKL | 5′-CAAACUUCCUGGUAACUCAdTdT-3′ |

### 2.12. NOX4 overexpression

Cells were electroporated with P5 primary cell Nucleofector™ Kit. For each transfection, cDNA (3 μg) was dissolved in 82 μL nucleofector solution, then added 18 μL supplemented P5 primary cell solution. Approximately $10^7$–$10^8$ cells were resuspended in 100 μL cDNA plus P5 primary cell solution and immediately electroporated in a 4D-Nucleofector X Kit L cuvette. Electroporated cells were transferred to 6-well plates containing 2.5 mL warm complete medium at 37 °C in a humidified atmosphere of 5% $CO_2$. After 24 h, the medium was replaced with fresh medium.

### 2.13. Western blotting assay

Briefly, the total protein was extracted after different treatments and the protein contents in each sample were determined by BCA™ Protein Assay Kit (Thermo Fisher). 30 μg proteins were subjected to SDS-PAGE and transferred onto PVDF membranes. After blocking with 5% non-fat milk in TBST at room temperature for 1 h, the membranes were incubated with specific primary antibodies and secondary antibodies. Bands were detected with SuperSignal West Femto Maximum Sensitivity Substrate (Pierce Biotechnology) and imaged with the ChemiDoc™ MP Imaging System (Bio-Rad, Hercules, CA, USA).

### 2.14. Statistical analysis

Data were expressed as the means ± SD. The differences between groups were analyzed using Prism 5.0 (Graph Pad Software Inc, San Diego, CA) and the statistical analysis was performed by analysis of variance (one-way ANOVA) followed by Student Newman-Keuls test. $p < 0.05$ is considered statistically significant.

## 3. Results

### 3.1. T-$BHP_L$ induced caspase-dependent endothelial apoptosis

MTT and alamarBlue assays showed that t-BHP significantly decreased cell viability in a dose- and time-dependent manner (Figs. 1A and B). T-$BHP_L$ (50 μM, 1 h)-induced endothelial acute and slight death was significantly reversed by Z-VAD-FMK, a pan-apoptosis inhibitor (Fig. 1C). The MTT results were further confirmed by Annexin V-7AAD staining by flow cytometry (Fig. 1D). Furthermore, t-$BHP_L$ treatment induced cleavage of caspase 3 and caspase 7 and decreased expression of Bcl-2, which were also reversed by Z-VAD-FMK (Fig. 1E).

### 3.2. T-$BHP_L$ activated endothelial NADPH oxidase

Compared with control group, t-$BHP_L$ induced intracellular ROS generation, which was dramatically suppressed by NAC (Fig. 2A). Meanwhile, NAC completely inhibited t-$BHP_L$-induced activation of caspase 3 and caspase 7 (Fig. 2B). To explore the sources of ROS, several inhibitors were applied. As shown in Fig. 2C, t-$BHP_L$-induced ROS was dramatically inhibited by DPI while ALL, Rot, TTFA, and AA showed no obvious effect. As NOX4 was one of the most important NADPH isoforms in endothelial cells contributing for ROS production [14], its role was investigated. Protein expression of total NOX4 was up-regulated by t-$BHP_L$ (Fig. 2E) Furthermore, western blotting and immunofluorescence revealed that NOX4 was localized and increased both on the membrane (Figs. 2F and G) and in the nucleus (Figs. 2F and H). In addition, the expression of p22phox, an essential adaptor protein for functional NOX4, was also increased by t-$BHP_L$ (Fig. 2D).

### 3.3. NOX4 played dual roles in endothelial apoptosis induced by t-$BHP_L$

To further confirm the role of NOX4 in t-$BHP_L$-induced cell apoptosis, NOX4 was silenced with NOX4 siRNA (Fig. 3A), inhibited with NOX4 inhibitor GKT137831 (Fig. 3B) or overexpressed by plasmid (Fig. 3F). ROS generation in response to t-$BHP_L$ was significantly decreased in NOX4 silenced and GKT137831 treated groups (Figs. 3C and D) but dramatically increased in NOX4 overexpression group (Fig. 3G). Furthermore, silence and inhibition of NOX4 dramatically protected endothelial cells against t-$BHP_L$-induced caspases activation (Fig. 3E). Interestingly, NOX4 overexpression significantly inhibited t-$BHP_L$-induced caspases activation as well (Fig. 3H). To further explore the mechanism, Akt-dependent survival pathway was investigated. T-$BHP_L$ exhibited no effect on Akt phosphorylation in normal cells but persistently increased in NOX4-overexpressed cells (Figs. 3I and J). In addition, in normal cells, Akt inhibitor VIII had no effect on t-$BHP_L$-induced caspases activation (Fig. 3K). However, in NOX4 overexpression cells, Akt inhibitor VIII significantly counteracted the inhibitory effect of NOX4 overexpression on caspase activation in response to t-$BHP_L$ (Fig. 3K).

### 3.4. P38MAPK mediated t-$BHP_L$-induced endothelial apoptosis

The mitogen-activated protein kinases (MAPKs), a family of kinases including extracellular signal-regulated kinases (ERKs), c-Jun N-terminal kinases (JNKs), and p38MAPKs, have been identified to be sensitive to oxidative stress and play critical roles in cell survival, proliferation, and death [15]. T-$BHP_L$ induced sustained phosphorylation of p38MAPK as well as transient phosphorylation of JNK1/2 and ERK1/2 (Fig. 4A). To identify the contribution of these kinases, inhibition of phosphorylation was achieved by SB203580, SP600125, and U0126, respectively (Fig. 4B). However, only SB203580 demonstrated significant inhibitory effect on t-$BHP_L$-induced caspase 3/7 activation (Fig. 4C).

### 3.5. T-$BHP_H$ induced endothelial necroptosis

T-$BHP_H$ (500 μM) induced higher cell death rate which could not be reversed by Z-VAD-FMK pretreatment (Fig. 5A). Translucent cytoplasm was observed even under microscopy (Fig. 5B). Significant increase in LDH release (Fig. 5C) and PI uptake (Fig. 5D) were also detected. Interestingly, the LDH release in response to t-$BHP_H$ was significantly reversed by RIP1 inhibitor Nec-1 and MLKL inhibitor NSA. However, compared with Nec-1 and NSA alone, no enhanced

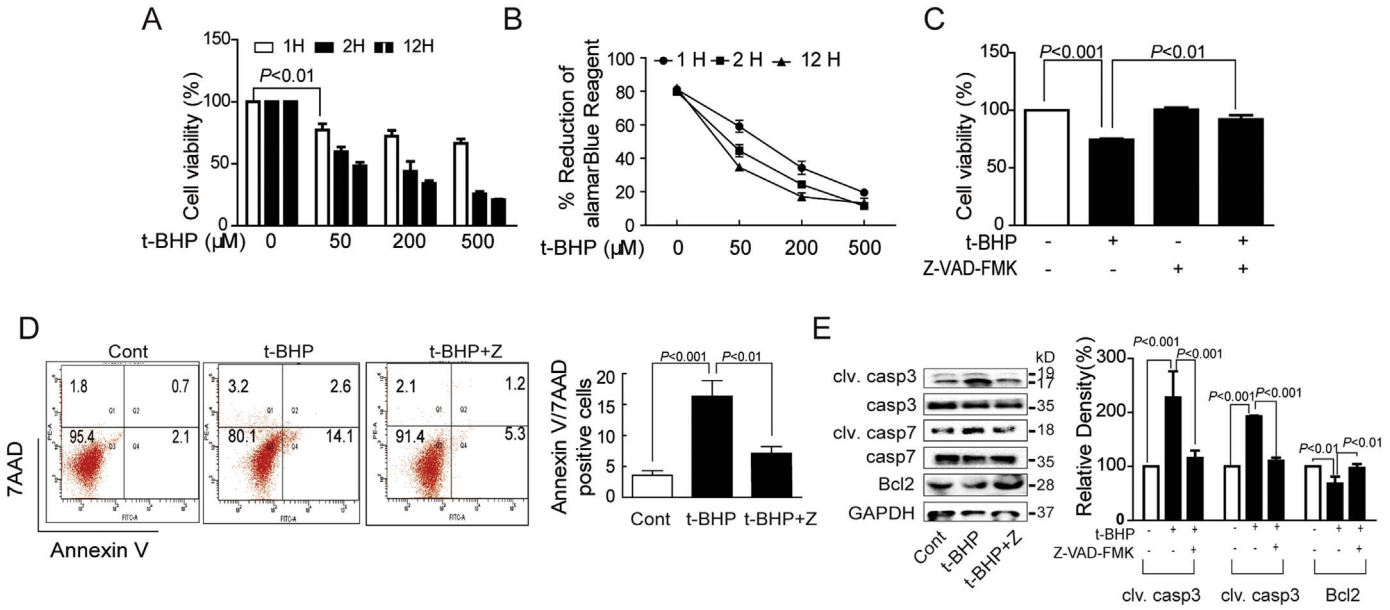


**Fig. 1.** T-$BHP_L$ induced caspase-dependent endothelial apoptosis. After treatment with a range of concentrations (50, 200, 500 μM) and time intervals (1, 2, 12 h) of t-BHP, the cell viabilities were tested by both MTT assay (A) and AlamarBlue assay (B). Endothelial cells were exposed to t-BHP (50 μM) for 1 h with or without Z-VAD-FMK (1 μM) pretreatment for 1 h, the cell viability, the apoptotic rate, and the expression of caspase 3, caspase 7, and Bcl-2 were was detected by MTT assay (C), Annexin V-7AAD staining (D) and Western blotting (E), respectively. The results were expressed as mean ± SD of three independent experiments. Cont, control group; Z, ZVAD-FMK.

protective effect was observed (Fig. 5E).

### 3.6. T-$BHP_H$ induced endothelial necroptosis via RIP1-RIP3-MLKL pathway

Necroptosis was mainly mediated by the RIP1-RIP3-MLKL signaling pathways [3,4]. Compared with the control group, t-$BHP_H$ enhanced the interaction of RIP1 and RIP3 (Fig. 6A) and increased phosphorylation of MLKL (Fig. 6B). When RIP1, RIP3, and MLKL were silenced by siRNAs (Fig. 6C), t-$BHP_H$-induced LDH release was significantly inhibited (Fig. 6D).

### 3.7. Mitochondrial ROS was required for t-$BHP_H$-induced necroptosis

The role of mitochondrial ROS in t-$BHP_H$-induced endothelial necroptosis was further investigated. Compared with t-$BHP_L$, t-$BHP_H$ induced much higher ROS generation (Fig. 7A), which could be inhibited by Rot, TTFA, and AA while DPI showed no effect (Fig. 7B). Rot, TTFA, and AA decreased t-$BHP_H$-induced LDH release as well (Fig. 7C). To explore the mitochondrial dysfunction induced by t-$BHP_H$, the MMP was monitored by fluorescence dye JC-1. The decreased red fluorescence and increased green fluorescence indicated the decrease of MMP. T-$BHP_H$-induced MMP decrease was partially reversed by RIP1 and RIP3 siRNA but not by MLKL siRNA (Fig. 7D). Furthermore, the mitochondrial ROS generation was detected by fluorescence probe MitoSox and the mitochondria were localized with MitoTracker. Silence RIP1 or RIP3 with siRNAs dramatically inhibited mitochondrial ROS generation in response to t-$BHP_H$ while MLKL siRNA showed no effect (Fig. 7E). In addition, t-$BHP_H$-induced RIP1-RIP3 interaction was dramatically inhibited by Rot, TTFA, and AA as determined by immunoprecipitation assay (Fig. 7G). However, MLKL phosphorylation was dramatically inhibited by TTFA, and AA but not by Rot as detected by western blotting (Fig. 7H).

### 3.8. P38MAPK was involved in t-$BHP_H$-induced endothelial necroptosis

The roles of MAPKs in t-$BHP_H$-induced endothelial necroptosis was investigated as well. T-$BHP_H$ also activated JNK1/2, ERK1/2, and p38MAPK. Nec-1 decreased t-$BHP_H$-induced p38MAPK phosphorylation while showed no effect on either ERK1/2 or JNK1/2 phosphorylation (Fig. 8A). Furthermore, t-$BHP_H$-induced p38MAPK phosphorylation was significantly inhibited by RIP1 and MLKL siRNAs (Fig. 8B). In addition, SB203580 significantly inhibited t-$BHP_H$-induced endothelial death as determined by MTT but showed no effect on LDH release (Figs. 8C and D).

## 4. Discussion

In this study, the cytotoxic effect of t-BHP on endothelial cells was investigated. The major findings include: 1) T-BHP induced endothelial apoptosis and necroptosis, which was dependent on concentration. 2) NOX4 played dual roles in t-$BHP_L$-induced endothelial death. 3) ROS from NOX4 and mitochondria differentially regulated endothelial apoptosis and necroptosis in response to t-$BHP_L$ and t-$BHP_H$, respectively. 4) P38MAPK actively participated in t-BHP-induced endothelial apoptosis and necroptosis.

Endothelial dysfunction caused by injury or death has been implicated in the pathogenesis of a variety of cardiovascular diseases [6,16]. Oxidative stress, resulted from the excessive generation of ROS, induced endothelial death has been well established. The major type of endothelial death was apoptosis while other types of non-apoptotic death such as necrosis were existed. T-BHP, an alternative to $H_2O_2$, induced dramatically endothelial death in a dose- and time-dependent manner. Compared with long-term oxidative stress, the roles of short-term oxidative stress in most physiological and pathological processes are controversial [17]. To explore the effect of short-term oxidative stress on endothelial cells, acute damage was induced by short-term stimulus with different concentrations of t-BHP. As expected, low concentration of t-BHP (t-$BHP_L$) (50 μM) induced endothelial caspase-mediated apoptosis as evidenced by the increased caspase cleavage, Annexin V/7AAD double staining and the inhibitory effect of Z-VAD-FMK, a pan-caspase inhibitor. Necroptosis, a regulated necrosis, demonstrates characteristics morphologically and biochemically different to that of apoptosis. Translucent cytoplasm, swelling of organelles, rapture of cell membrane, etc have been considered as the morphological characteristics of necrosis/necroptosis while the activation of RIP1-RIP3-MLKL has been identified as the main molecular mechan-

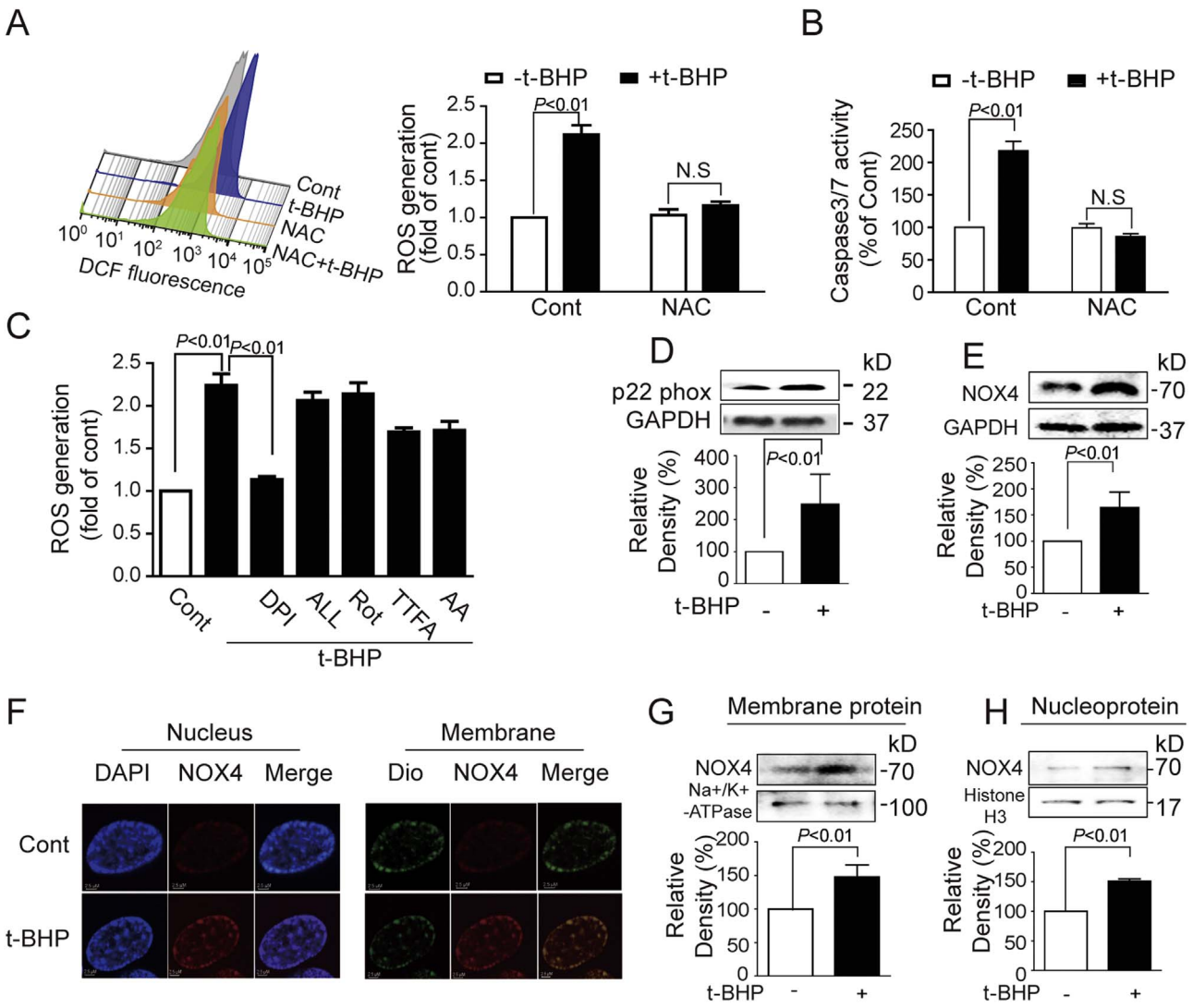


**Fig. 2.** T-$BHP_L$ activated endothelial NADPH oxidase Endothelial cells were treated with t-BHP (50 μM) for 1 h with or without NAC (5 mM), Rot (20 μM), TTFA (10 μM), AA (5 μM), DPI (1 μM), ALL (10 μM) pretreatment 1 h. ROS production were evaluated by DCF (A and C) and apoptosis was detected by caspase 3/7 Activity Assay Kit (B). Cells were treated with t-$BHP_L$ for 1 h, the total, membrane and nucleus proteins were isolated. The expression of total NOX4 and p22 phox was detected by Western blotting (D and E). The location expression of NOX4 on membrane and in nucleus was detected with immunofluorescence (F) and Western blotting (G and H). Results were expressed as mean ± SD of three independent experiments. AA, antimycin A; ALL, allopurinol; Cont, control group; DPI, diphenyleneiodonium; NAC, N-acetyl-L-cysteine; ROS, reactive oxygen species; Rot, rotenone; TTFA, 2-thenoyltrifluoroacetone.

isms for necroptosis [2–4]. High concentration of t-BHP (t-$BHP_H$) (500 μM) induced LDH release and PI uptake suggesting the rapture of the cell membrane. The cell death induced by t-$BHP_H$ was not reversed by Z-VAD-FMK but by Nec-1, an inhibitor for RIP1, and NSA, an inhibitor for MLKL. Together with the translucent cytoplasm, these results suggested that t-$BHP_H$ induced necroptosis in endothelial cells. The increased interaction between RIP1 and RIP3, increased MLKL phosphorylation, and the inhibitory effect of RIP1, RIP3, MLKL siRNAs on cell death revealed that necroptosis was mediated by RIP1-RIP3-MLKL pathway. Previous report showed that $H_2O_2$ induced iron-dependent necrosis in L929sAhFas cells [18]. This might be mainly due to the difference in cell genotype as L929sAhFas was a Fas gene transfected cell line while cells used in this study was primary endothelial cells.

Increased ROS generation in endothelial cells induced apoptosis [5]. T-$BHP_L$-induced ROS formation in endothelial cells was inhibited by NAC. Furthermore, NAC nearly completely reversed t-$BHP_L$ induced caspase 3/7 activities suggesting that t-$BHP_L$-induced apoptosis was mediated by ROS. NADPH oxidase and mitochondria are two main sources of ROS in endothelial cells [7,8]. T-$BHP_L$-induced ROS generation was inhibited by DPI, a NADPH oxidase inhibitor but mitochondrial respiratory chain inhibitors failed to do so suggesting that ROS was from NADPH oxidase in t-$BHP_L$ treated cells. NOX4, one of the 7 isoforms of the NADPH oxidase, is considered as the most important ROS-producing enzyme in endothelial cells and plays a vital role in regulating endothelial cell survival and death [19,20]. However, the biological roles of NOX4 in the cardiovascular system remain elusive [21,22]. Here, we found that t-$BHP_L$ induced NOX4 expression accompanied by the increased expression of p22phox, an essential component for NOX4 activation [23,24]. Silencing of NOX4 significantly inhibited ROS formation and the pro-apoptotic effects of t-$BHP_L$, which was consistent with previous findings in renal and lung epithelial cells [25,26]. In contrast to the pro-apoptotic effects of NOX4, some studies indicated that increased NOX4 expression could increase cell viability [27,28]. Here, in NOX4-overexpressing cells, increased NOX4 caused more ROS production but indeed exhibited inhibitory effects on t-$BHP_L$-induced endothelial death. To explore the mechanism for this phenomenon, role of Akt, an important pro-survival signal pathway in many cells [29–31], was examined. T-$BHP_L$ had no effect on Akt phosphorylation and inhibition of Akt showed no effect on t-$BHP_L$-induced apoptosis in

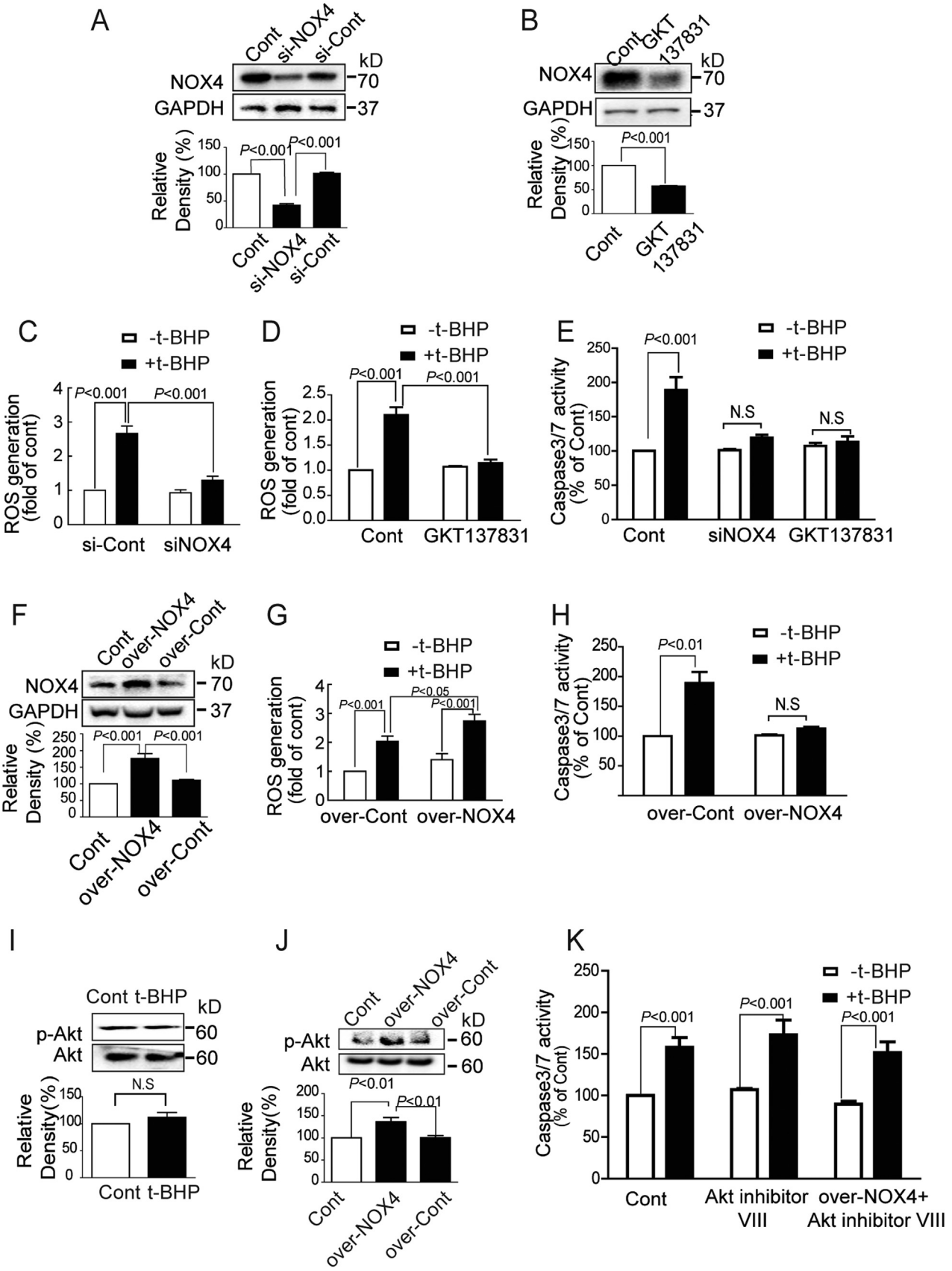


**Fig. 3.** NOX4 played dual roles in endothelial apoptosis induced by t-$BHP_L$ NOX4 was knocked down by siNOX4 (A), inhibited by GKT137831 (10 nM) (B), or overexpressed by NOX4 plasmid (over-NOX4) (F), the ROS production (C, D, and G) and the caspase 3/7 activities (E and H) in response to t-$BHP_L$ were determined. The Akt and p-Akt protein expression in normal (I) and NOX4 overexpressed (J) cells in response to t-$BHP_L$ were determined by Western blotting. NOX4 overexpressed cells were treated with t-$BHP_L$ for 1 h with or without Akt inhibitor VIII (5 μM) pretreatment for 1 h and the caspase 3/7 activities were detected by caspase 3/7 Activity Assay Kit (K). The results were expressed as mean ± SD of three independent experiments. ROS, reactive oxygen species; Cont, control group.

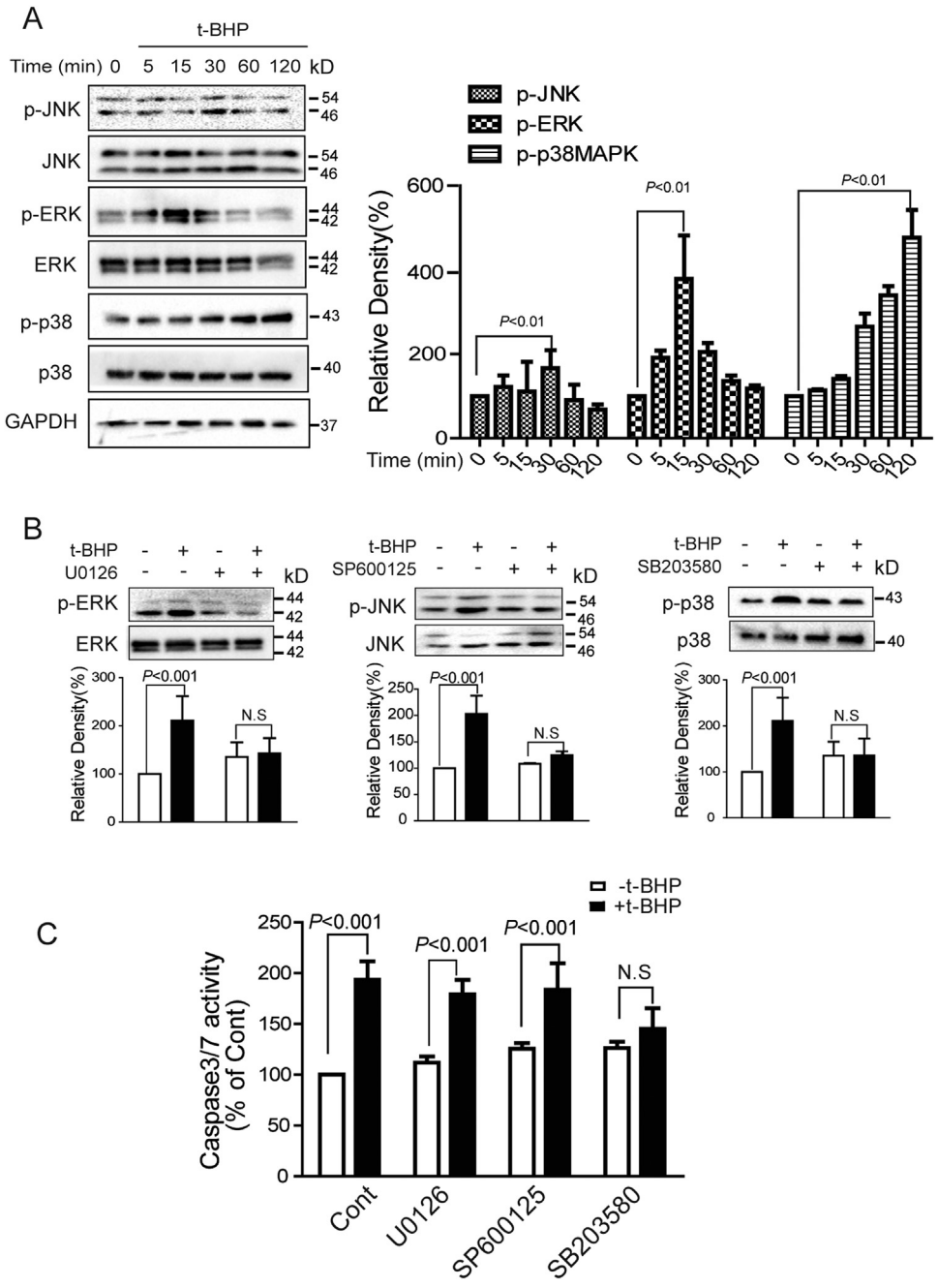


**Fig. 4.** P38MAPK mediated t-BHP$_L$-induced endothelial apoptosis Endothelial cells were treated with t-BHP$_L$ and the phosphorylation of JNK1/2, p38MAPK, and ERK1/2 were detected by Western blotting (A). Cells were treated with t-BHP$_L$ for 1 h with or without U0126 (1 μM), SP600125 (1 μM), or SB203580 (1 μM) pretreatment for 1 h, the expression of MAPKs was detected by Western blotting (B) and the caspase 3/7 activities were detected by caspase 3/7 Activity Assay Kit (C). The results were expressed as mean ± SD of three independent experiments. N.S, no significance.

normal endothelial cells. However, in NOX4-overexpressing cells, Akt was activated and protected against t-BHP$_L$-induced endothelial death. This protective effect was partially reversed by Akt inhibitor VIII suggesting that Akt played a pro-survival role in this process. Although both t-BHP$_L$ and NOX4 overexpression increased NOX4 expression in endothelial cells, they demonstrated differential effects on cell survival. This seemingly contradictory results might due to the fact that low levels of ROS have no or very weak effect on the activation of Akt while high levels of ROS dramatically activate Akt by increased mitochondrial metabolism [32,33]. In our study, the levels of ROS generation induced by NOX4 overexpression were much higher those of t-BHP$_L$-induced ROS in endothelial cells.

As ROS was also actively involved in necroptosis induced by stimulus such as TNF [34], and small molecules dimethyl fumarate [35,36] etc, its roles in t-BHP induced necroptosis were further explored. T-BHP$_H$ induced ROS formation was inhibited by mitochondrial respiratory chain inhibitors but not by NADPH oxidase inhibitor suggesting that mitochondria could be the main source of ROS. The decreased LDH release and RIP1-RIP3 interaction by mitochondrial respiratory chain inhibitors also suggested the participation of mitochondria. The specific role of mitochondria in necroptosis remains unclear [37]. RIP1 was reported to be involved in TNF-α-induced ROS formation and necroptosis through interaction with NADPH oxidase while the role of RIP3 remains unclear [38]. Here, we found that mitochondrial respiratory chain inhibitors affect the RIP1-RIP3 interaction and MLKL phosphorylation suggesting that mitochondria might

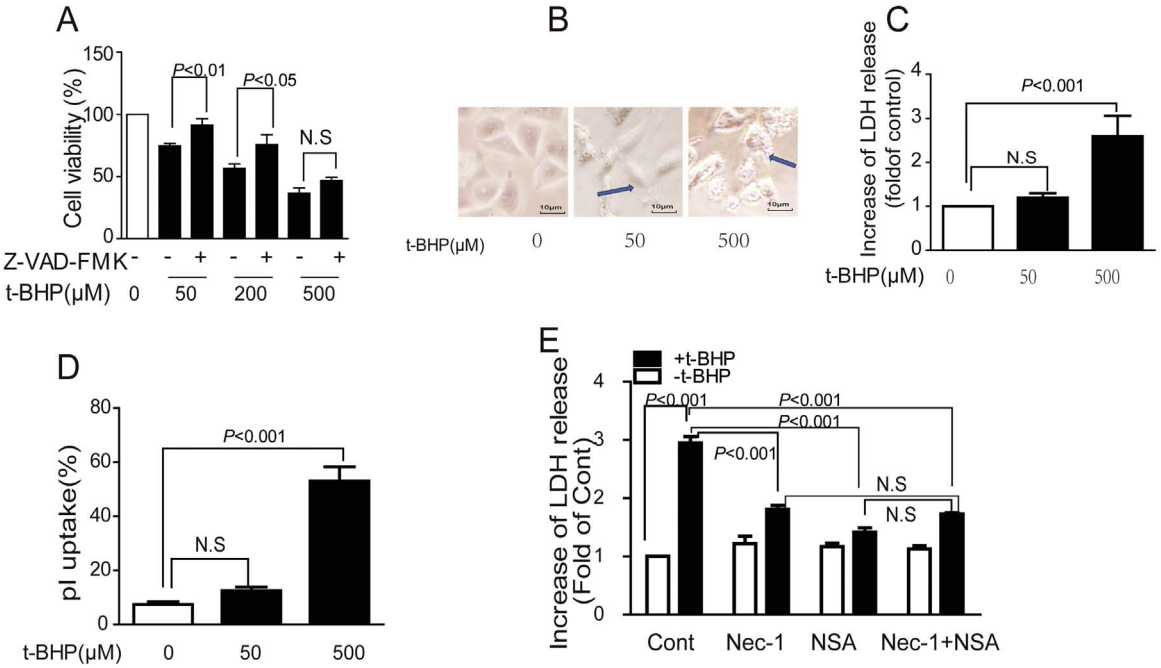


**Fig. 5.** T-BHP$_H$ induced endothelial necroptosis Endothelial cells were incubated with t-BHP (0–500 μM) for 1 h, the cell viability, morphological alterations, LDH release, and the PI uptake were detected by MTT assay (A), microscopy (B), LDH assay kit (C), and PI staining (D), respectively. Cell were treated with t-BHP$_H$ for 1 h with Nec-1 (1 μM) and NSA (1 μM) alone or co-treatment for 1 h. The cell viability was examined by LDH assay kit (E). Results were expressed as mean ± SD of three independent experiments. Nec-1, necrostatin-1; NSA, necrosulfonamide.

regulate necroptosis through ROS formation. However, silence RIP1 and RIP3 could inhibit t-BHP$_H$-induced MMP decrease and mitochondria ROS formation while silence MLKL showed no effect. Thus, there might be a reciprocal regulatory feedback between RIP/RIP3 and the mitochondria ROS in response to t-BHP$_H$. These data suggested that ROS from different sources might determine the death types in endothelial cell in response to t-BHP insults.

MAPKs are well-established redox sensitive mediators actively involved in regulating cell death [39–41]. JNK and p38MAPK contribute to endothelial apoptosis in response to oxidative stress, TNF,

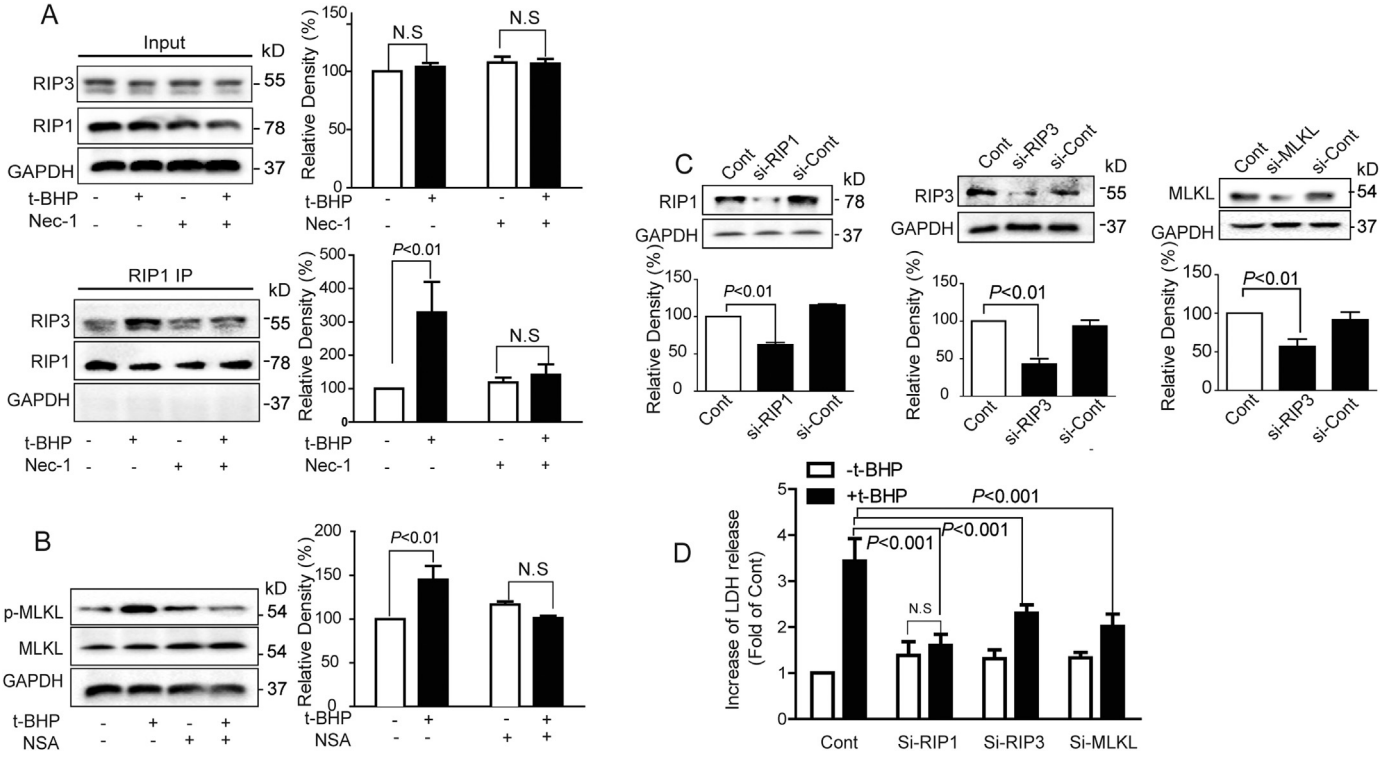


**Fig. 6.** T-BHP$_H$ induced endothelial necroptosis through RIP1-RIP3-MLKL Endothelial cells were treated with t-BHP$_H$ for 1 h with or without Nec-1 (1 μM) pretreatment for 1 h, the interaction of RIP1 and RIP3, and the phosphorylation of MLKL were detected by immunoprecipitation (A) and Western blotting (B), respectively. RIP1, RIP3, and MLKL were silenced by siRNAs (C), the cell viability in response to t-BHP$_H$ for 1 h was detected by LDH assay kit (D). The results were expressed as mean ± SD of three independent experiments. Cont, control group.

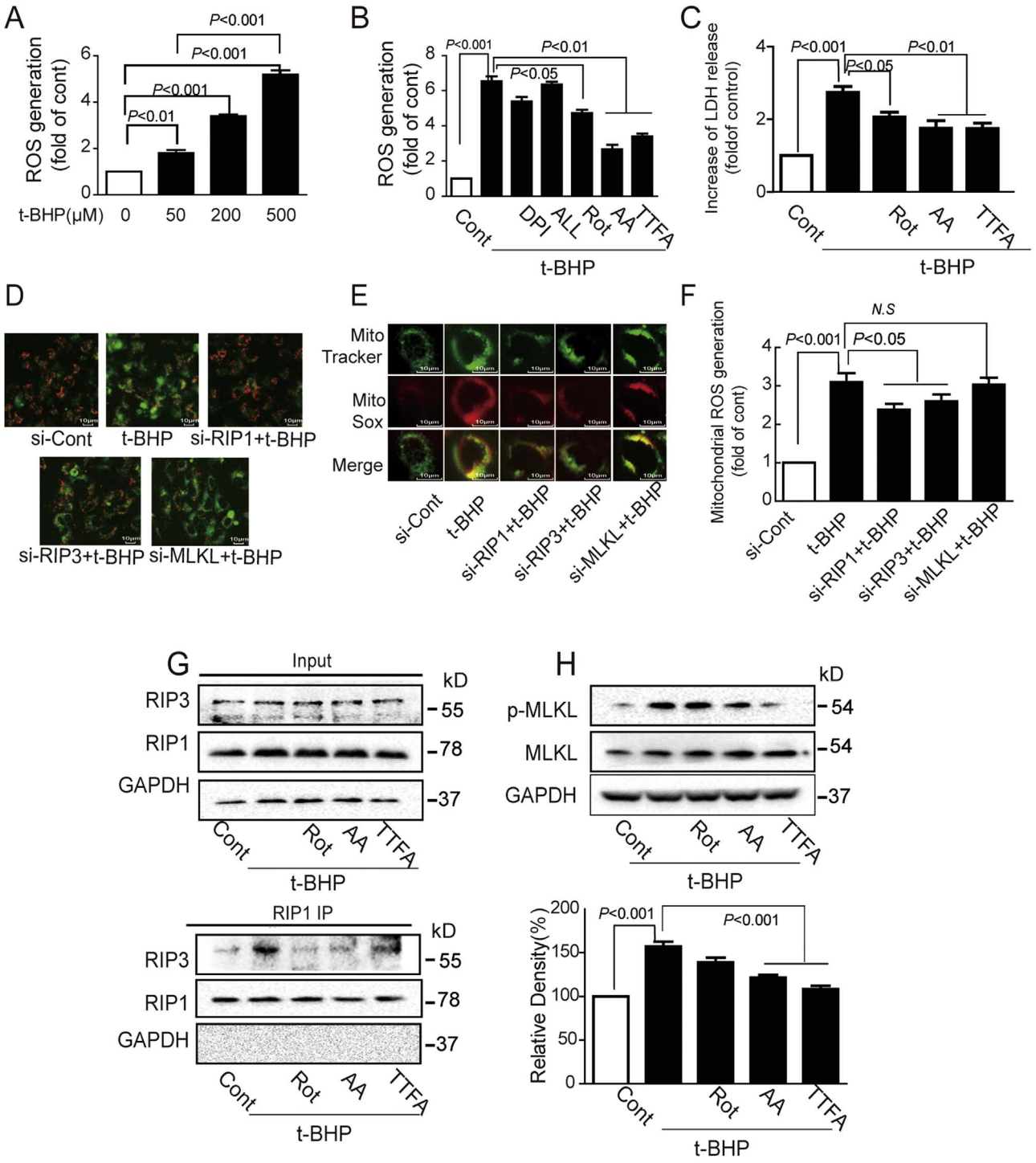


**Fig. 7.** Mitochondrial ROS was required for activation of t-$BHP_H$-induced endothelial necroptosis. Endothelial cells were treated with t-BHP (50–500 μM) 1 h with or without Rot (20 μM), TTFA (10 μM), AA (5 μM) pretreatment for 1 h, ROS generation and LDH release were detected by flow cytometer (A and B) and LDH assay kit (C). After transfected with RIP1, RIP3, or MLKL siRNAs, cells were treated with t-$BHP_H$ for 15 min. The MMP and mitochondrial ROS generation were detected with JC-1 staining (D) and MitoSOX by fluorescence microscopy (E) and detected by FACScan flow cytometer (F). Cells were treated with t-$BHP_H$ for 1 h with or without Rot (20 μM), TTFA (10 μM), AA (5 μM) pretreatment for 1 h, RIP1-RIP3 interaction and MLKL phosphorylation were detected by immunoprecipitation (G) and Western blotting (H). The results were expressed as mean ± SD of three independent experiments. AA, antimycin A; ALL, allopurinol; Cont, control group; DPI, diphenyleneiodonium; LDH, lactate dehydrogenase; MMP, mitochondrial membrane potential; ROS, reactive oxygen species; Rot, rotenone; TTFA, 2-thenoyltrifluoroacetone.

endoplasmic reticulum stress, genotoxic stress etc [5]. Prolonged JNK activation was required for TNF-induced necroptosis in L929 cells [42]. In this study, although JNK, p38MAPK, and ERK were activated by both t-$BHP_L$ and t-$BHP_H$, only the p38MAPK inhibitor SB203580 reversed t-BHP's cytotoxicity. The inhibitory effect of Nec-1, RIP1 siRNA, and MLKL siRNA on t-$BHP_H$-induced p38MAPK expression provided further evidence for its involvement in necroptosis. Thus, p38MAPK might serve as a pro-death effector regardless of cell death types in t-BHP treated endothelial cells.

Taken together, as depicted in Fig. 8E, the present study showed that t-$BHP_L$ induced caspase-dependent apoptosis while necroptosis occurred after cells were treated with t-$BHP_H$. ROS derived from

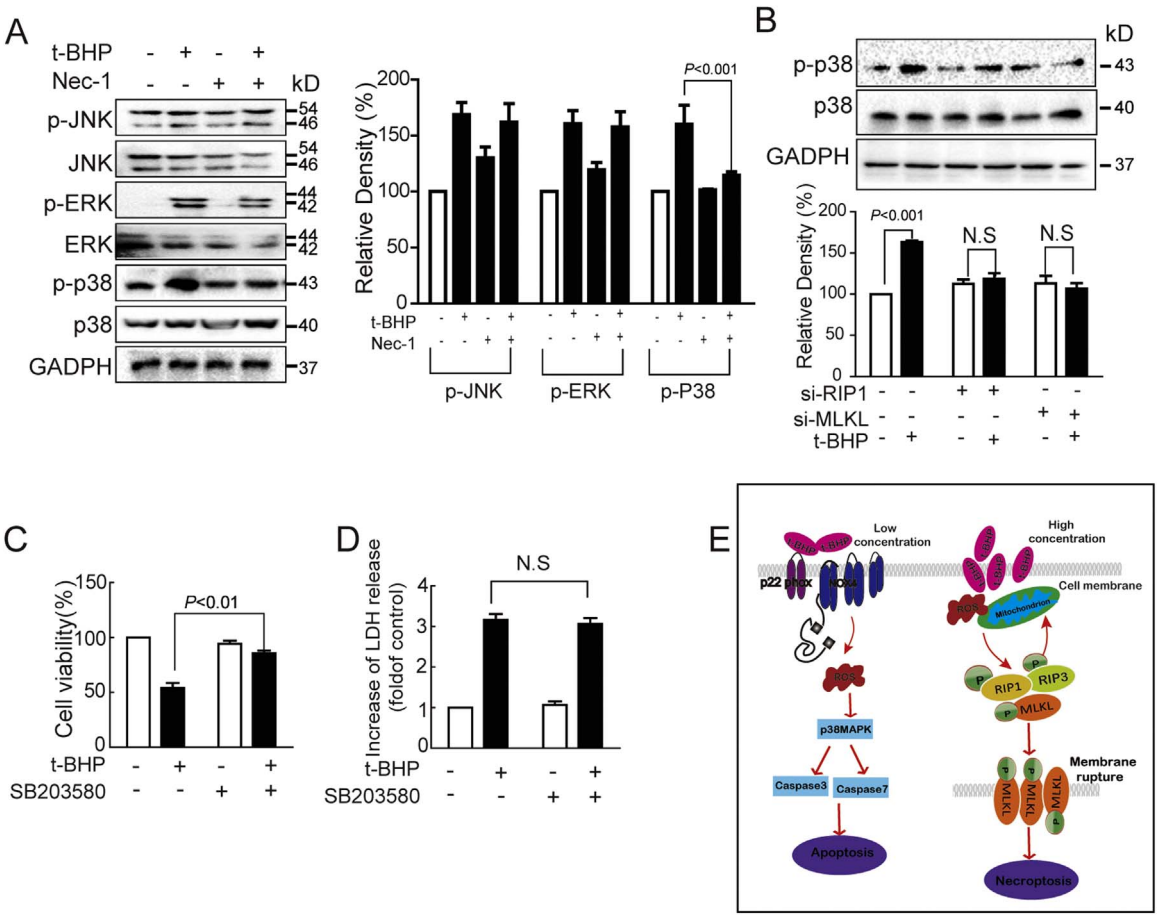


**Fig. 8.** P38MAPK was involved in t-BHP$_H$-induced endothelial necroptosis Endothelial cells were treated with t-BHP$_H$ for 15 min with or without Nec-1 (1 μM) pretreatment for 1 h, expressions of total and phosphorylated JNK1/2, p38MAPK and ERK1/2 were detected by Western blotting (A). Endothelial cells transfected with siRNA against RIP1 or MLKL were treated with t-BHP$_H$ for 15 min, the expression of phosphorylated p38MAPK was analyzed by Western blotting (B). Endothelial cells were treated t-BHP$_H$ for 1 h with or without SB203580 (1 μM) pretreatment for 1 h, the cell viability and the LDH release were examined by MTT assay (C) and LDH assay kit (D), respectively. (E) Hypothetical signal pathway of t-BHP-induced endothelial apoptosis and necroptosis in endothelial cells. These results were expressed as mean ± SD of three independent experiments. LDH, lactate dehydrogenase;Nec-1, necrostatin-1.

NADPH oxidase and mitochondria played important roles in t-BHP-induced apoptosis and necroptosis, respectively. These results provided the possibility of exploring novel therapeutic agents targeting organelle-based ROS for the improvement of endothelial death and related vascular diseases.

## Disclosures

We declare that none of the authors has any kind of conflict of interest related to the present work.

## Acknowledgments

This study was supported by the Science and Technology Development Fund of Macau Special Administrative Region (039/2014/A1) and the Research Fund of University of Macau (MYRG2016-00043-ICMS-QRCM).

## References

[1] A. Ashkenazi, G. Salvesen, Regulated cell death: signaling and mechanisms, Annu. Rev. Cell Dev. Biol. 30 (2014) 337–356.
[2] P. Vandenabeele, et al., Molecular mechanisms of necroptosis: an ordered cellular explosion, Nat. Rev. Mol. Cell Biol. 11 (10) (2010) 700–714.
[3] T. Vanden Berghe, et al., Regulated necrosis: the expanding network of non-apoptotic cell death pathways, Nat. Rev. Mol. Cell Biol. 15 (2) (2014) 135–147.
[4] M. Conrad, et al., Regulated necrosis: disease relevance and therapeutic opportunities, Nat. Rev. Drug Discov. 15 (5) (2016) 348–366.
[5] J.S. Pober, W. Min, J.R. Bradley, Mechanisms of endothelial dysfunction, injury, and death, Annu. Rev. Pathol. 4 (2009) 71–95.
[6] J.B. Su, Vascular endothelial dysfunction and pharmacological treatment, World J. Cardiol. 7 (11) (2015) 719–741.
[7] E. Panieri, M.M. Santoro, ROS signaling and redox biology in endothelial cells, Cell Mol. Life Sci. 72 (17) (2015) 3281–3303.
[8] R.S. Frey, M. Ushio-Fukai, A.B. Malik, NADPH oxidase-dependent signaling in endothelial cells: role in physiology and pathophysiology, Antioxid. Redox Signal. 11 (4) (2009) 791–810.
[9] J. Zhao, et al., Mixed lineage kinase domain-like is a key receptor interacting protein 3 downstream component of TNF-induced necrosis, Proc. Natl. Acad. Sci. USA 109 (14) (2012) 5322–5327.
[10] S.W. Yu, et al., Mediation of poly(ADP-ribose) polymerase-1-dependent cell death by apoptosis-inducing factor, Science 297 (5579) (2002) 259–263.
[11] N. Vanlangenakker, T. Vanden Berghe, P. Vandenabeele, Many stimuli pull the necrotic trigger, an overview, Cell Death Differ. 19 (1) (2012) 75–86.
[12] V.V. Nikolaychik, M.M. Samet, P.I. Lelkes, A new method for continual quantitation of viable cells on endothelialized polyurethanes, J. Biomater. Sci. Polym. J. Biomater. Sci. Polym. Ed. 7 (10) (1996) 881–891.
[13] W. Zhao, C. Wu, X. Chen, Cryptotanshinone inhibits oxidized LDL-induced adhesion molecule expression via ROS dependent NF-kappaB pathways, Cell Adh. Migr. (2015) 0.
[14] T. Ago, et al., Nox4 as the major catalytic component of an endothelial NAD(P)H oxidase, Circulation 109 (2) (2004) 227–233.
[15] Y. Son, et al., Mitogen-activated protein kinases and reactive oxygen species: how can ROS activate MAPK pathways?, J. Signal. Transduct. (2011) 792639.
[16] A. Daiber, et al., Targeting vascular (endothelial) dysfunction, Br. J. Pharmacol. (2016).
[17] D. Gems, L. Partridge, Stress-response hormesis and aging: "that which does not kill us makes us stronger", Cell Metab. 7 (3) (2008) 200–203.
[18] T. Vanden Berghe, et al., Necroptosis, necrosis and secondary necrosis converge on similar cellular disintegration features, Cell Death Differ. 17 (6) (2010) 922–930.
[19] F. Yan, et al., Nox4 and redox signaling mediate TGF-beta-induced endothelial cell

apoptosis and phenotypic switch, Cell Death Dis. (2014) 5.
[20] S. Basuroy, et al., Nox4 NADPH oxidase mediates oxidative stress and apoptosis caused by TNF-alpha in cerebral vascular endothelial cells, FASEB J. (2009) 23.
[21] R.M. Touyz, A.C. Montezano, Vascular Nox4: a multifarious NADPH oxidase, Circ. Res. 110 (9) (2012) 1159–1161.
[22] F.J. Miller Jr., Nox4 NADPH oxidase: emerging from the veil of darkness, Eur. Heart J. (2015).
[23] M.C. Dinauer, et al., Human neutrophil cytochrome b light chain (p22-phox). Gene structure, chromosomal location, and mutations in cytochrome-negative autosomal recessive chronic granulomatous disease, J. Clin. Investig. 86 (5) (1990) 1729–1737.
[24] G. Zalba, et al., NADPH oxidase-dependent superoxide production is associated with carotid intima-media thickness in subjects free of clinical atherosclerotic disease, Arterioscler. Thromb. Vasc. Biol. 25 (7) (2005) 1452–1457.
[25] D. Amatore, et al., Influenza virus replication in lung epithelial cells depends on redox-sensitive pathways activated by NOX4-derived ROS, Cell Microbiol. 17 (1) (2015) 131–145.
[26] J. Chen, J.K. Chen, R.C. Harris, Angiotensin II induces epithelial-to-mesenchymal transition in renal epithelial cells through reactive oxygen species/Src/caveolin-mediated activation of an epidermal growth factor receptor-extracellular signal-regulated kinase signaling pathway, Mol. Cell Biol. 32 (5) (2012) 981–991.
[27] S. Basuroy, et al., Nox4 NADPH oxidase-derived reactive oxygen species, via endogenous carbon monoxide, promote survival of brain endothelial cells during TNF-alpha-induced apoptosis, Am. J. Physiol. Cell Physiol. 300 (2) (2011) C256–C265.
[28] K. Schroder, et al., Nox4 is a protective reactive oxygen species generating vascular NADPH oxidase, Circul. Res. 110 (9) (2012) 1217.
[29] D.A. Altomare, A.R. Khaled, Homeostasis and the importance for a balance between AKT/mTOR activity and intracellular signaling, Curr. Med. Chem. 19 (22) (2012) 3748–3762.
[30] S.R. Datta, et al., Akt phosphorylation of BAD couples survival signals to the cell-intrinsic death machinery, Cell 91 (2) (1997) 231–241.
[31] G. Song, G.L. Ouyang, S.D. Bao, The activation of Akt/PKB signaling pathway and cell survival, J. Cell. Mol. Med. 9 (1) (2005) 59–71.
[32] I. Dey-Guha, et al., Asymmetric cancer cell division regulated by AKT, Proc. Natl. Acad. Sci. USA 108 (31) (2011) 12845–12850.
[33] V. Nogueira, N. Hay, Molecular pathways: reactive oxygen species homeostasis in cancer cells and implications for cancer therapy, Clin. Cancer Res. 19 (16) (2013) 4309–4314.
[34] H. Blaser, et al., TNF and ROS crosstalk in inflammation, Trends Cell Biol. 26 (4) (2016) 249–261.
[35] X. Xie, et al., Dimethyl fumarate induces necroptosis in colon cancer cells through GSH depletion/ROS increase/MAPKs activation pathway, Br. J. Pharmacol. 172 (15) (2015) 3929–3943.
[36] W. Sun, et al., 2-Methoxy-6-acetyl-7-methyljuglone (MAM), a natural naphtho-quinone, induces NO-dependent apoptosis and necroptosis by H2O2-dependent JNK activation in cancer cells, Free Radic. Biol. Med. 92 (2016) 61–77.
[37] K.D. Marshall, C.P. Baines, Necroptosis: is there a role for mitochondria?, Front Physiol. 5 (2014) 323.
[38] P. Vandenabeele, et al., The role of the kinases RIP1 and RIP3 in TNF-induced necrosis, Sci Signal. 3 (115) (2010) re4.
[39] M.L. Circu, T.Y. Aw, Reactive oxygen species, cellular redox systems, and apoptosis, Free Radic. Biol. Med. 48 (6) (2010) 749–762.
[40] J. Zwerina, et al., Activation of p38 MAPK is a key step in tumor necrosis factor-mediated inflammatory bone destruction, Arthritis Rheum. 54 (2) (2006) 463–472.
[41] J.Y. Lee, B.P. Yu, H.Y. Chung, Activation mechanisms of endothelial NF-kappa B, IKK, and MAP kinase by tert-butyl hydroperoxide, Free Radic. Res. 39 (4) (2005) 399–409.
[42] Y.S. Kim, et al., TNF-induced activation of the Nox1 NADPH oxidase and its role in the induction of necrotic cell death, Mol. Cell 26 (5) (2007) 675–687.